CHEMMEDCHEM

CHEMISTRY ENABLING DRUG DISCOVERY

Accepted Article

Title: Design, synthesis and structure-activity relationship analysis of novel thiazolo[3,2-a]pyrimidin derivatives with anti-inflammatory activity in acute lung injury

Authors: Guang Liang, Lingfeng Chen, Yiyi Jin, Weitao Fu, Siyang Xiao, Chen Feng, Bo Fang, Yugui Gu, Chenglong Li, Yunjie Zhao, and Zhiguo Liu

To be cited as: *ChemMedChem* 10.1002/cmdc.201700175

Link to VoR: http://dx.doi.org/10.1002/cmdc.201700175

A Journal of

ChemPubSoc Europe

WILEY-VCH

www.chemmedchem.org

Design, synthesis and structure-activity relationship analysis of novel thiazolo[3,2-a]pyrimidin derivatives with anti-inflammatory activity in acute lung injury

Lingfeng Chen[ab1], Yiyi Jin[a1], Weitao Fu[a], Siyang Xiao[a], Chen Feng[a], Bo Fang[a], Yugui Gu[c], Chenglong Li[a], Yunjie Zhao[a]*, Zhiguo Liu[a]*, Guang Liang[ab]*

[1] These authors contributed equally to this work.

[a] Dr. L. Chen, Y. Jin, Dr. W. Fu, S. Xiao, C. Feng, B. Fang, Prof. C. Li, Prof. Y. Zhao, Prof. Z. Liu, Prof. G. Liang.
Chemical Biology Research Center, School of Pharmaceutical Sciences, Wenzhou Medical University, Wenzhou, Zhejiang 325035, China

[b] Dr. L. Chen, Prof. G. Liang.
School of Chemical Engineering, Nanjing University of Science and Technology, Nanjing, Jiangsu, 210094, China

[c] Prof. Y. Gu
School of Chemical Engineering and Materials, Wenzhou University, Wenzhou, Zhejiang 325035, China

* Corresponding author:
Guang Liang, Ph.D, Professor
Chemical Biology Research Center at School of Pharmaceutical Sciences, Wenzhou Medical University. 1210 University Town, Wenzhou, Zhejiang 325035, China
Tel: (+86)-577-86699396; Fax: (+86)-577-86699396.
E-mail: wzmcliangguang@163.com

and

Zhiguo Liu, Ph.D, Associate Professor, E-mail: lzgcnu@163.com
Yunjie Zhao, Ph.D, Associate Professor, E-mail: aabye1100@yahoo.com.cn

Abstract

Acute lung injury (ALI) results in high lethality rate, and interleukin-6 (IL-6) and tumor necrosis factor-α (TNF-α) contribute most to tissue deterioration in ALI. In this study, we designed and synthesized a new series of thiazolo[3,2-a]pyrimidine derivatives based on lead compound found previously, and evaluated their anti-inflammatory activities. The structure-activity relationship studies led to the discovery of two highly potent inhibitors. Two promising compounds inhibited lipopolysaccharide (LPS)-induced IL-6 and TNF-α release in a dose-dependent manner in mouse primary peritoneal macrophages (MPMs). Furthermore, administration of them resulted in lung histopathological improvements and attenuated LPS-caused ALI *in vivo*. Taken together, these data indicate that the novel thiazolo[3, 2-a]pyrimidine derivatives could be developed as candidates for the treatment of ALI.

Keywords: Thiazolo[3,2-a]pyrimidines; Acute lung injury; Anti-inflammatory; Cytokines; interleukins;

1. Introduction

Acute lung injury (ALI) is characterized by non-cardiogenic pulmonary edema, and results in several disorders including pneumonia, aspiration syndromes, sepsis, and major trauma and shock.[1] Despite advancing knowledge, lethality from ALI remains high (30-40%), which is comparable to that of breast cancer.[1c, 2] Although several pharmacologic treatments have been developed, such as protease inhibitors, glucocorticoids, antioxidants, surfactants and anti-thrombotic treatments, none has proven to be effective.[3] Hence, the development of alternative strategies against ALI is highly desirable.

Several clinical studies have demonstrated that inflammatory cytokines play a crucial role in mediating the initiation and amplification of ALI. Two key cytokines, interleukin-6 (IL-6) and tumor necrosis factor-α (TNF-α) contribute most to the deterioration seen in ALI.[4] Elevated levels of IL-6 and TNF-α have been found in bronchoalveolar lavage fluid (BALF) from human or experimental ALI.[1c, 5] These observations suggest that attenuating excessive production of pro-inflammatory cytokines, including IL-6 and TNF-α, may be promising approach for ALI therapy. Inhibitors against the cytokine storm are emerging, and a few are effective in clinical applications.[6]

*Please insert **Figure 1** here*

Thiazolo- and pyrimidine-fused heterocyclic ring-systems were commonly found in novel therapeutics,[7] including antimicrobial (**1**, Figure 1),[8] antiviral (**2**), anticancer (**3**, **4**)[9], anti-Parkinson's (**5**),[10] and anti-inflammatory agents[11]. In the past, our research group has designed, synthesized and evaluated a number of compounds targeting pro-inflammatory cytokines for the treatment of sepsis and ALI.[12] Amongst these compounds, ethyl (Z)-7-methyl-2-(4-morpholinobenzylidene)-3-oxo-5-phenyl-2, 3-dihydro-5H-thiazolo[3,2-a]pyrimidine-6-carboxylate (**6**)[13] with a thiazolo- and pyrimidine-fused heterocyclic ring showed high inhibitory rate on the release of

cytokines such as IL-6 and TNF-α in a dose-dependent manner and exhibited a beneficial protection effects against liposaccharide (LPS)-induced septic death in a mouse model. Yet, the relationship between anti-inflammatory activity and thiazolo[3,2-a]pyrimidine derivatives remains unclear. Thus, we herein evaluated the anti-inflammatory properties of thiazolo[3,2-a]pyrimidine derivatives, their inhibitory effect against LPS-induced expression of IL-6 and TNF-α, as well as the structure−activity relationships.

2. Results and discussion

2.1 Chemistry

The synthesis route of thiazolo[3,2-a]pyrimidine derivatives is shown in Scheme 1 (**11a**-**o**) and Scheme 2 (**12a**-**i**). The dihydropyrimidine derivatives **8a**-**o** were prepared using the classic one pot Biginelli reaction[14] of commercially available ethyl 3-oxobutanoate, thiourea, and the corresponding aldehydes (**7a**-**o**), catalyzed by sulfamic acid. Subsequently, Biginelli product **(8a**-**o**) was refluxed with ethyl 2-chloroacetate in the presence of pyridine to afford the cyclization product **9a**-**o**. The nitrogen containing aldehydes **10a**-**f** and **13a** were obtained by nucleophilic displacement of the 4-fluorobenzaldehyde with the corresponding amines (Supporting Information Scheme S1).[15] **10g**-**i** were commercially available. Finally, cyclization products **9a**-**o** were allowed to undergo a Knoevenagel condensation with 4-morpholinobenzaldehyde (**13a**) to yield compounds **11a**-**o**. Similarly, reaction of ethyl 7-methyl-3-oxo-5-(thiophen-2-yl)-2,3-dihydro-5*H*-thiazolo[3,2-a]pyrimidine-6-carbo xylate (**9l**) with corresponding aldehydes **10a**-**i** provided compounds **12a**-**i**. The resulting residues were purified by silica chromatography and elution with 30% EtOAc in petroleum ether. Compounds were then recrystallized in EtOH and DCM solution (2:1) to yield target compounds at 35-85% (**11a**-**o**, **12a**-**i**). Analytical and spectral data of all synthesized compounds are in full agreement with the proposed structures.

*Please insert **Scheme 1** and **Scheme 2** here*

2.2 Screening for inhibitory effect against LPS-induced IL-6 and TNF-α release

LPS is one of the most potent innate immune-activating stimuli found in the outer membrane of Gram-negative bacteria. LPS induces the activation of monocytes and macrophages, resulting in the production of pro-inflammatory cytokines including TNF-α, IL-6, and IL-12.[16] Experimental and clinical evidence shows that pro-inflammatory cytokines play a significant role in the pathogenesis of inflammation-induced ALI. We utilized an enzyme-linked immunosorbent assay (ELISA) to screen for the inhibition of LPS-induced IL-6 and TNF-α release by the synthesized compounds (**11a-o**, **12a-i**) in mouse primary peritoneal macrophages (MPMs). Macrophages were pre-incubated with the compounds at 10 μM concentration for 30 min. Compound **6** was used as a positive control, and DMSO was the vehicle control. Following pretreatment, MPMs were challenged with LPS (0.5 μg/mL) for 24 h at 37 °C. The ability (% inhibition) of the detected compounds to reduce pro-inflammatory cytokines IL-6 and TNF-α is summarized in Table 1 and Table 2.

*Please insert **Table 1** and **Table 2** here*

Among these compounds, **11a**, **11b**, **11e**, **11i** and **11l** exhibited strong inhibition on IL-6 expression (inhibitory rates > 75%), whereas **11e**, **11f**, **11i**, **11n** and **12d** showed high inhibitory effect on TNF-α expression (inhibitory rates > 60%). Notably, **11e** and **11l**, with an 4-allyloxy phenyl and thiophen group at R^1 respectively, showed the strongest inhibitory effect on LPS-induced cytokine expression. For **11e** and **11l**, inhibitory rates reached 92.82% and 94.75% for IL-6, and 65.96% and 65.67% for TNF-α, respectively, compared to the LPS control.

2.3 Structure–activity relationship analysis of thiazolo[3,2-a]pyrimidin derivatives

To our knowledge, there are several studies showing thiazolo[4,5-d]pyrimidines

scaffold as anti-inflammatory agents, but few have reported on the cytokine-inhibitory effects of thiazolo[3,2-a]pyrimidine derivatives and their structure−activity relationship (SAR).[7] As shown in Table 1, compounds with halogen substitution on the phenyl moiety at the R^1-position such as 4-bromo (**11a**) or 4-fluoro (**11b**) group, showed similar potency to the lead compound **6** (phenyl). An improved activity was observed when the allyloxy group was introduced at the para-position of phenyl (**11e**, with 92.8 % and 65.96 % inhibitory rates for IL-6 and TNF-α, respectively). On the other hand, replacement of the phenyl group with 3,4-dimethoxyphenyl (**11c**) or 4-ethoxyphenyl (**11d**), slightly decreased the activity against IL-6. Incorporation of hydroxyl group at the meta- or para- position (**11f** and **11g**) led to significant reduction in the inhibition rates of IL-6 (67.9 % and 45.9 %, respectively), whereas TNF-α inhibitory activity remained comparable to **6**. Surprisingly, the introduction of 3,4-dihydroxyphenyl (**11i**) dramatically enhanced the activities against TNF-α (71.4 % inhibitory rates). But conversion of one hydroxy group of **11i** to a methoxy group at the para-position (**11h**) resulted in dramatic loss of IL-6 and TNF-α inhibitory activities. Furthermore, when a heterocyclic substitution was introduced at R^1-position, IL-6 inhibition displayed the following order: thiophen (**11l**, 94.7%) > 4-methylthiazol (**11j**, 37.2%) > 5-methylfuran (**11k**, 36.8%), and the activities of **11j** and **11k** against TNF-α decreased approximately 3-fold relative to **11l**. Compounds with nonaromatic substitution, such as compound **11m** (cyclopropyl), **11n** (propyl) and **11o** (cyclohexyl), showed significant loss of activities.

Compound **11l** exhibited a good overall profile and was selected to further optimize the R^2-position (Table 2). The introduction of 4-methylpiperazine and other nitrogen-containing substituents at the para-position of the phenyl ring led to compounds **12a-e**. We observed that **12a-d** lost the ability to inhibit IL-6 release. But **12d**, with a diethylamino group, showed the highest inhibitory activity against TNF-α (76.3% inhibitory rates). However, the removal of morpholinyl group (**12i**) resulted in total loss of ability against IL-6 and TNF-α, suggesting that the potency for suppressing IL-6 or TNF-α expression is directly related to the substituent at the para-position of phenyl and that the oxygen atom of morpholinyl group is

indispensable. Interestingly, the introduction of (dimethylamino)propoxy (**12h**) group caused a high level of toxicity in human normal hepatic cell line (HL-7702) at a concentration of 10 μM (30% relative survival). While other active compounds showed no significant toxicity in HL-7702 and MPMs after 24 h treatment (Supporting Information Figure. S1AB). Compounds with heterocyclic substitution at R^2-position (**12f** and **12g**), exhibited weak anti-inflammatory activity. To demonstrate the SAR of thiazolo[3,2-a]pyrimidin derivatives in the inhibition of IL-6 and TNF-α expression, quantitative SAR (QSAR) was constructed. The results of predicted versus experimental values are shown in Figure 2. The QSAR results indicate that the atomic mass may play an important role in the anti-IL-6 activity, while atomic charge and electro-negativity may influence the anti-TNF-α inhibitory activity. Taken together, the SAR and QSAR results on the IL-6 and TNF-α inhibitory activities of the thiazolo[3,2-a]pyrimidin derivatives may provide valuable information for further development of novel anti-inflammatory compounds.

*Please insert **Figure 2** here*

2.4 Active compounds inhibit TNF-a and IL-6 release in a dose-dependent manner

Based on significant inhibitory activities and lower cytotoxicity against HL-7702 cells than lead compound **6**, **11e**, **11f**, **11i** and **11l** were selected for further evaluation of dose-dependent inhibitory effects against LPS-induced IL-6 and TNF-α release. As shown in Figure 3A-B, all active compounds exhibited a dose-dependent inhibition of IL-6 and TNF-α induced by LPS. Most of the compounds potently suppressed the cytokines with IC_{50} values in the low micromolar range. Interestingly, **11e** and **11l** showed IC_{50} values in the nanomolar range. Their potency against TNF-α release were increased by 3-5x fold compared to compound **6**. These results suggest that **11e** and **11l** are promising anti-inflammatory candidates for the treatment of acute inflammatory diseases such as ALI and sepsis.

*Please insert **Figure 3** here*

*2.5 Effect of **11e** and **11l** pretreatment on survival rate in mice after LPS administration*

Sepsis is a systemic inflammatory response to infections and is often fatal.[17] LPS from Gram-negative bacteria has been implicated as a major cause of sepsis. To determine whether active compounds are able to attenuate the development of inflammatory shock *in vivo*, LPS was intraperitoneally (i.p.) injected into mice at 20 mg/kg with or without **11e** and **11l** pretreatment. Survival rate of mice was then monitored for 7 days. As shown in Figure 4, all mice in the LPS control group died within 36 h as a result of sepsis. By contrast, 40% and 30% of the animals that received **11e** and **11l** respectively, at 20 mg/kg prior to LPS injection survived. The overall difference in survival rate between **11e** and **11l** treated group and control group was significant ($p < 0.01$). Thus, both of the compounds showed excellent anti-inflammatory activity *in vivo*.

*Please insert **Figure 4** here*

*2.6 Compounds **11e** and **11l** ameliorated histopathological changes in lung tissues following LPS challenge*

Thiazolo[3,2-a]pyrimidin derivatives **11e** and **11l** were also evaluated in mice with ALI induced by intratracheal instillation of LPS. As shown in Figure 5A, the lung wet/dry weight ratio, an index of lung edema,[18] was significantly suppressed in LPS + **11e** or **11l** group when compared to the LPS alone group. Figure 5B also shows that LPS challenge remarkably increased the total number of cells in mice bronchial alveolar lavage fluid (BALF), whereas treatment with **11e** and **11l** at 10 and 20 mg/kg significantly decreased the numbers. In addition, recruitment of neutrophils into the lung tissue is an important factor in causing tissue damage in ALI.[19] As shown in Figure S2, LPS challenge substantially increased the number of neutrophils, whereas treatment with **11e** and **11l** resulted in significantly lower number of neutrophils in BALF.

To verify the inhibitory effect of **11e** and **11l** against macrophage infiltration into

the lung tissue, we performed immunofluorescence detection for CD68. CD68 is a glycoprotein which binds to low density lipoprotein and is highly expressed on monocytes/macrophages.[20] As shown in Figure 5D, LPS induced a significant accumulation of CD68-positive cells in the lung sections (red fluorescence). On the other hand, with **11e** and **11l** pretreatment, no notable change in CD68-positive macrophages were observed when compared to the control group. The quantification of CD68 staining fluorescence is shown in Figure 5C. We then evaluated the histological changes after **11e** and **11l** treatment in LPS-challenged mice by hematoxylin and eosin (H&E) staining. Lung tissues from the control group mice showed a normal structure, while LPS instillation resulted in significant alterations characterized by interstitial edema, pulmonary congestion, infiltration of inflammatory cells and thickening of the alveolar wall. However, these pathological changes induced by LPS were remarkably ameliorated by 20 mg/kg of **11e** and **11l** treatment (Figure 5E). These studies show that **11e** and **11l** had a remarkable protective effect on LPS-induced histopathological changes in a rat model of ALI.

*Please insert **Figure 5** here*

*2.7 Attenuation of acute LPS-induced pulmonary inflammation by **11e** and **11l***

Pro-inflammatory cytokines, including IL-6 and TNF-α, are known to play a critical role in the early phase of ALI. Thus, the levels of pro-inflammatory cytokines were measured in BALF and serum to confirm the inhibitory effect of **11e** and **11l** *in vivo*. As shown in Figure 6, cytokine levels were significantly elevated after LPS challenge compared to control mice. Administration of **11e** and **11l** at a dose of 20 mg/kg significantly reduced the levels of IL-6 and TNF-α in BALF as well as in serum samples. These results indicated that **11e** and **11l** had a protective effect on LPS-induced pulmonary inflammation of ALI.

*Please insert **Figure 6** here*

*2.8 Compounds **11e** and **11l** suppressed LPS-induced mRNA expression in Mice*

LPS exposure also increased the mRNA levels of inflammatory cytokines in mouse lung tissues.[21] Therefore, we next investigated the inhibitory effect of compounds **11e** and **11l** on mRNA abundance of important pro-inflammatory factors, including IL-1β, IL-6, TNF-α, vascular cell adhesion molecule 1 (VCAM-1) and intercellular adhesion molecule-1 (ICAM-1) in the mouse model of ALI. As shown in Figure 7, **11e** and **11l** at 10 mg/kg and 20 mg/kg effectively suppressed LPS-induced upregulation of mRNA of various cytokines in a dose-dependent manner. These data showed that anti-inflammatory compounds **11e** and **11l** partly affect the cytokine profile at the mRNA level.

*Please insert **Figure 7** here*

3. Conclusion

ALI is a major cause of acute respiratory failure in patients with no effective treatment.[22] Hence, there is a pressing need to identify an effective strategy to prevent or mitigate ALI. Thiazolo and pyrimidine fused heterocyclic rings are viable templates for the development of anti-inflammatory molecules.[7] In this study, we designed and synthesized a novel series of thiazolo[3,2-a]pyrimidine analogues and evaluated their anti-inflammatory activity relative to the lead compound **6**. The majority of the synthetic analogues exhibited significant inhibitory activities against LPS-induced TNF-α and IL-6 expression in MPMs. The preliminary structure−activity relationship (SAR) studies indicated that an electron donating group such as allyloxy at the para-position of the phenyl group or heterocycles such as thiophen at R^1 enhances anti-inflammatory activity. Further optimization of R^2 position indicates that oxygen atom of morpholinyl group is crucial to maintain the activity. Following initial screening for anti-inflammatory activity, **11e** and **11l** were identified as the most promising compounds. Pretreatment with **11e** and **11l** decreased the W/D ratio and the cytokines levels in BALF and serum of animals challenged with LPS. More importantly, **11e** and **11l** ameliorated the histopathological changes of lung and suppressed the mRNA levels of multiple inflammatory factors in LPS stimulated ALI mice. Taken together, **11e** and **11l** are promising potential

anti-inflammatory candidates for the treatment of ALI.

4. Experimental section

4.1. Chemistry

In general, commercial chemicals or solvents were reagent grade and were used without further purification. All reagents for synthesis were obtained from Sigma Aldrich and Energy-Chemical. All reactions were monitored by thin-layer chromatography (250 silica gel 60 F_{254} glass plates). Melting points were determined on a Fisher-Johns melting apparatus and were uncorrected. ^{1}H NMR and ^{13}C NMR spectra were recorded on a Bruker 600 MHz instruments, and the chemical shifts were presented in terms of parts per million with TMS as the internal reference. *J* values are given in hertz. The spectra data of the target compounds were shown in Supporting Information. Electronspray ionization mass spectra in positive mode (ESI-MS) data were obtained with a Bruker Esquire 3000t spectrometer. Chromatographic purification was carried out on Silica Gel 60 (E.Merck, 70-230 mesh). Analytical HPLC analyses were performed on Agilent 1260 liquid chromatograph fitted with a Inertex C18 column (4.6 mm×150 mm, 5 μm particle size) with CH_3CN-H_2O (A) and 0.1% TFA in CH_3CN-H_2O (B) solvent mixtures and equipped with a G1314AVWD detector. The purity of all synthetic compounds was determined by HPLC analysis and was greater than 95%.

*4.1.1. General procedure for the preparation of the intermediates **8a-o***

Sulfamic acid (3 mmol) was added to a solution of benzaldehydes **7a-o** (2 mmol), ethyl acetylacetate (2.5 mmol), and thiourea (3 mmol) in ethanol (30 mL) and refluxed for 4 h. The mixture was cooled to room temperature and poured to water. The residue was filtered and washed with 10% MeOH in water to give crude products (**8a-o**) in 52.0-93.4 % yield.

*4.1.2. General procedure for the preparation of the intermediates **9a-o***

Crude product (**8a-o**, 2 mmol) was refluxed with ethyl 2-chloroacetate (2.5 mmol)

in the presence of pyridine (1 mmol) in ethanol (20 mL) for 3 hours to afford the cyclization crude solution of **9a**-**o**.

*4.1.3. General procedure for the preparation of the aminobenzaldehydes intermediates **10a-f, 13a***

Example: 4-((2-(dimethylamino)ethyl)(methyl)amino)benzaldehyde (**10e**). A mixture of 4-Fluorobenzaldehyde (620.5 mg, 5 mmol), N^1, N^1, N^2-trimethylethane-1,2-diamine (766.3 mg, 7.50 mmol) and K_2CO_3(1.38 g, 10 mmol) was stirred in dry DMF at 100°C under nitrogen atmosphere overnight. Then the reaction was quenched by addition of water. The resulting mixture was extracted with EtOAc (3 × 25 mL), washed with brine, dried over anhydrous Na_2SO_4 and concentrated. The resulting residue was purified by flash chromatography (Yield 45.8 %). ^{1}H NMR (600 MHz, DMSO-d_6) δ (ppm): 9.649 (s, 1H, -CHO), 7.668 (d, J = 9.0 Hz, 2H, Ar-H), 6.778 (d, J = 9.0 Hz, 2H, Ar-H), 3.528 (t, J = 7.2 Hz, 2H, N-C$\underline{H}_2$-CH$_2$-), 3.021 (s, 3H, C$\underline{H}_3$-N-CH$_2$-CH$_2$-), 2.399 (t, J = 7.2 Hz, 2H, N-CH$_2$-C$\underline{H}_2$-), 2.184 (s, 6H, N-CH$_2$-CH$_2$-N(C$\underline{H}_3$)$_2$). ^{13}C NMR (150 MHz, DMSO-d_6) δ (ppm): 189.70, 153.27, 131.70×2, 124.43, 110.90×2, 55.67, 49.54, 45.52×2, 38.39. ESI-MS m/z: 207.3 $(M + H)^+$, calcd for $C_{12}H_{18}N_2O$: 206.14. The characterization of other aldehydes were reported in the Supporting Information file.

*4.1.4.1. General Procedure for the Preparation of the Thiazolo[3, 2-a]pyrimidines **11a-o**, **12a-i*** Example: ethyl(Z)-5-(4-bromophenyl)-7-methyl-2-(4-morpholinobenzylidene)-3-oxo-2,3-dihydro-5*H*-thiazolo[3,2-a]pyrimidine-6-carboxylate (**11a**): 4-(4-methylpiperazin-1-yl)benzaldehyde (2 mmol) was added to a solution of crude 9a described above in the presence of morpholine (1 mmol) to undergo a Knoevenagel condensation in EtOH, and the mixture was stirred at 78 °C for 6 h. Then the mixture was diluted with EtOAc (50 mL) and washed with water (2 × 50 mL) and saturated brine (50 mL). The solution was dried ($MgSO_4$) and concentrated in vacuo. The crude product was purified by silica chromatography eluting with 30 %

EtOAc in petroleum ether and recrystallized to afford **11a** as red powder (56.5% yield). m.p: 162.5-163.9 ºC, 98% purity. ^{1}H NMR (600 MHz, DMSO-d_6) δ (ppm): 7.676 (s, 1H, C=CH-Ph), 7.547 (d, J = 8.4 Hz, 2H, Ar-H), 7.464 (d, J =9.0 Hz, 2H, Ar-H), 7.256 (d, J = 8.4 Hz, 2H, Ar-H), 7.058 (d, J = 9.0 Hz, 2H, Ar-H), 6.008 (s, 1H, pyrimidine-H), 4.026-4.047 (m, 2H, $CH_3C\underline{H}_2O$-), 3.721 (t, J = 4.8 Hz, 4H, morpholine), 3.295 (t, J = 4.8 Hz, 4H, morpholine), 2.384 (s, 3H, pyrimidine-CH_3), 1.124 (t, J = 7.2 Hz, 3H, $C\underline{H}_3CH_2O$-). ^{13}C NMR (150 MHz, DMSO-d_6) δ (ppm): 164.77, 164.47, 156.16, 152.24, 152.02, 139.89, 133.82, 132.084×2, 131.58×2, 129.69 ×2, 122.04, 121.68, 114.12×2, 113.41, 107.59, 65.78×2, 60.15, 54.28, 46.64×2, 22.53, 13.87. ESI-MS m/z: 569.2 $(M + H)^+$, calcd for $C_{27}H_{26}BrN_3O_4S$: 567.08. Other target compounds **11b**-**11o**, **12a**-**12i** can be found in the Supporting Information.

4.2 Animals

Male C57BL/6 mice and Institute of Cancer Research (ICR) mice weighing 18 to 22 g were obtained from the Animal Center of Wenzhou Medical University (Wenzhou, China). The animals were acclimatized in an air-conditioned room and maintained in a 12:12-h light/dark cycle and fed with standard food and water. Animals involved in this experiment were treated in accordance with the Guide for Care and Use of Laboratory Animals of National Institutes of Health. The present study was approved by Wenzhou Medical College Animal Policy and Welfare Committee (approval documents: 2013/APWC/0361).

4.3 Cells and reagents

Lipopolysaccharide (LPS) was purchased from Sigma-Aldrich (St Louis, MO, USA). The mouse IL-6 and TNF-α enzyme-linked immunosorbent assay (ELISA) kits were obtained from eBioscience, Inc. (San Diego, CA, USA). For peritoneal macrophage preparation, ICR mice were stimulated by intraperitoneal (i.p.) injection of 3 mL thioglycollate solution (Beef extract (0.3 g), tryptone (1 g), sodium chloride (0.5 g) and soluble starch (6 g) which were dissolved and boiled in 100 mL water. The

solution was filtrated with 0.22 mm filter per mouse and kept in pathogen-free conditions for 3 days before peritoneal macrophage isolation. Total peritoneal macrophages were harvested by washing the peritoneal cavity with PBS containing 30 mM of EDTA (8 mL per mouse) and centrifuged. The pellet was resuspended in RPMI-1640 medium (Gibco/BRL life Technologies, Eggenstein, Germany) with 10% FBS (Hyclone, Logan, UT), 100 U/mL penicillin and 100 mg/mL streptomycin. Peritoneal macrophages were cultured on 60 mm plates ($1.2*10^6$ cells in 3 mL media per plate) and maintained at 37 ^oC in a 5% CO_2-humidified air. Nonadherent cells were removed by washing with medium for 3 h after seeding. Experiments were undertaken after the cells adhered firmly to the culture plates.

4.4 Determination of IL-6 and TNF-α

The inhibition effects of IL-6 and TNF-α release of novel thiazolo[3,2-a]pyrimidin derivatives were evaluated in LPS stimulated MPMs. After treatment of cells with indicated compounds and LPS, the cytokines levels in medium were determined by an ELISA kit (eBioScience, San Diego, CA) according to the manufacturer's instructions. Briefly, MPMs were seeded into 96-well plates at a density of 400000 cells per well in DMEM medium and incubated at 37 °C in 5% CO_2 for 24 h. Cells were pretreated with compounds for 30 min, and then LPS was added (0.5 μg/mL). After 24 h, the culture media and cells were collected separately. The total protein in cultural plates was collected and the concentrations were determined by using Bio-Rad protein assay. The total amount of the inflammatory factor in the media was normalized to the total protein quantity of the viable cell pellets.

4.5 Real-Time quantitative PCR

Cells were homogenized in TRIZOL kit (Invitrogen, Carlsbad, CA) for extraction of RNA according to each manufacturer's protocol. Both reverse transcription and quantitative PCR were carried out using a two-step M-MLVPlatinum SYBR Green qPCR SuperMix-UDG kit (Invitrogen, Carlsbad, CA).

Eppendorf Mastercycler ep realplex detection system (Eppendorf, Hamburg, Germany) was used for q-PCR analysis. The primers of genes including IL-1β, IL-6, TNF-α, VCAM-1, ICAM-1 and β-actin were synthesized by Invitrogen. The primer sequences of mouse genes used are shown as follows:

Mouse β-actin sense primer, CCGTGAAAAGATGACCCAGA;

Mouse β-actin antisense primer, TACGACCAGAGGCATACAG.

Mouse TNF-α sense primer, TGATCCGCGACGTGGAA;

Mouse TNF-α antisense primer, ACCGCCTGGAGTTCTGGAA.

Mouse IL-6 sense primer, GAGGATACCACTCCCAACAGACC;

Mouse IL-6 antisense primer, AAGTGCATCATCGTTGTTCATACA.

Mouse IL-1β sense primer, ACTCCTTAGTCCTCGGCCA;

Mouse IL-1β antisense primer, CCATCAGAGGCAAGGAGGAA.

Mouse VCAM-1 sense primer, TGCCGAGCTAAATTACACATTG;

Mouse VCAM-1 antisense primer, CCTTGTGGAGGGATGTACAGA.

Mouse ICAM-1 sense primer, GCCTTGGTAGAGGTGACTGAG;

Mouse ICAM-1 antisense primer, GACCGGAGCTGAAAAGTTGTA.

The amount of each gene was determined and normalized by the amount of β-actin.

4.6 Assessment of cytotoxicity of active compounds

To assess the safety of the thiazolo[3, 2-a]pyrimidine derivatives. Compounds were tested for their totoxicity in the human normal hepatic cell line (HL-7702) or MPMs by MTT at a concentration of 10 μM. The survival rates of the cells with the administrated compounds at 24 h were determined.

4.7 Quantitative structure-activity relationships analysis

4.7.1 Quantitative SAR (QSAR) model

These thiazolo[3, 2-a]pyrimidine derivatives were calculated with the ChemoPy descriptor calculation program [40]. In this program, about 1000 molecular

descriptors based on molecular structure were obtained. After calculation, those molecular descriptors that stayed constant for all molecules were eliminated and pairs of variables with a correlation coefficient greater than 0.75 were classified as inter-correlated and one in each correlated pair was deleted.

4.7.2 Multiple linear regression (MLR) analysis

MLR analysis is a statistical method that uses several explanatory variables to predict the outcome of a response variable. The goal of multiple linear regression (MLR) is to model the relationship between the explanatory and response variables. In present study, MLR was performed using R program, a widely used tool for statistical computing and graphics, to derive QSAR models. The biological data used in this study were the IL-6 or TNF-α inhibitory rates in comparison to LPS alone group. The inhibition rates against IL-6 and TNF-α release were used as dependent variables in the linearization procedure. Subsequently, Stepwise Multiple Linear Regression (Stepwise-MLR) was applied to select the significant descriptors. The most relevant descriptors were used as independent variables.

4.7.3 Validation of the models

Validation of the lineal models are required for testing the predictive ability and generalizing the methods by cross-validation. The leave-one-out (LOO) procedure was employed. When a data point was removed from the analyzed set, the regression was recalculated, and then the predicted value for that point was compared to its actual value. This process was repeated until each datum had been omitted once and then the sum of squares of these deletion residuals could be used to calculate q^2, an equivalent statistic to R^2.

4.8. Lipopolysaccharide-induced sepsis in Mice

Compounds 11e and 11l were dissolved in 0.1% sodium carboxyl methyl cellulose (CMC-Na). Male ICR mice were pretreated with 11e, 11l or vehicle for seven days by intragastric administration (20 mg/kg/day), followed by the injection of

LPS (i.v., 20 mg/kg). Control animals received same volume (200 μL) of vehicle. Mortality were recorded for 7 days at an interval of 12 h after the LPS injection.

4.9. LPS-induced ALI

Male B6 mice were randomly divided into six groups, designated control (n = 6), LPS (n = 6), and **11e** (10 mg/kg and 20 mg/kg) + LPS (n = 6) and **11l** (10 mg/kg and 20 mg/kg) + LPS (n = 6). Prior to intratracheal injection of LPS (5 mg/kg), the mice were treated orally with **11e** and **11l** at a dose of 10 mg/kg or 20 mg/kg for 1 week. After 6 h of LPS induction, mice were then euthanized with ketamine. The chest cavity of each animal was carefully opened, and the collection of BALF was performed.

4.10. Wet-to-dry weight ratio

The lung wet/dry weight ratio was calculated to observe the pulmonary edema. Mice were sacrificed at 6 h after LPS challenge. After the middle lobe of right lung was collected, the wet weight was recorded. Then lung was heated in a thermostatic oven at 65 °C for 48 h and weighed to determine the baseline lung dry mass levels.

4.11. Protein concentration in bronchoalveolar lavage fluid (BALF)

Collected BALF was centrifuged at 1000 rpm for 10 min at 4 °C, and the supernatant was used for protein concentration and cytokine determinations. The precipitation was resuspended in 50 μL physiological saline. The total number of cells on BALF was detected by cell counting instrument. The protein concentration in the supernatant was determined by using a BCA protein assay (Pierce, Rockford, IL, USA).

4.12. Histopathologic examination of lung

The superior lobe of right lung was collected and fixed in 4% formalin solution, and then embedded in paraffin and cut into 5 μm sections. After dehydration, the sections were stained with hematoxylin and eosin (H&E) using standard protocol and

observed with a Nikon Eclipse E800 microscope (400× amplification; Nikon, Tokyo, Japan).

4.13. Immunofluorescence for CD68 detection

After deparaffinization and rehydration, 5 μm lung sections were treated with 3% H_2O_2 for 20 min and with 1% BSA in PBS for 30 min. Slides were incubated overnight at 4 °C with anti-CD68 antibody (Santa Cruz; 1:100), and then incubated with PE-labeled secondary antibody (Santa Cruz;1:200) for 1 h at room temperature. Following staining the nucleus with DAPI for 5 min, the images were viewed under confocal microscope (400×, amplification; Nikon A1, Japan).

4.14. Statistical analysis

Results are presented as the mean ± standard error of the mean (SEM). Student's t test or ANOVA multiple comparisons were employed to analyze the statistical significance of differences between sets of data. Statistics was performed using GraphPad Pro (GraphPad, San Diego, CA). P values less than 0.05 were considered significant. All experiments were repeated at least three times.

Conflict of interest

The authors have declared no conflict of interest.

Acknowledgment

Financial support was provided by the National Natural Science Foundation of China (21572167, 21572166, and 81622043), Natural Science Foundation of Zhejiang Province (LR16H310001 and LY17B020008), and Xinmiao Talent Program of Zhejiang Province (2015R413081 and 2016R413063).

References

[1] a) O. Brattstrom, F. Granath, P. Rossi, A. Oldner, *Acta Anaesthesiol Scand* **2010**, *54*, 1007-1017; b) C. Brun-Buisson, C. Minelli, G. Bertolini, L. Brazzi, J. Pimentel, K. Lewandowski, J. Bion, J. A. Romand, J. Villar, A. Thorsteinsson,

P. Damas, A. Armaganidis, F. Lemaire, A. S. Group, *Intensive Care Med* **2004**, *30*, 51-61; c) G. D. Rubenfeld, E. Caldwell, E. Peabody, J. Weaver, D. P. Martin, M. Neff, E. J. Stern, L. D. Hudson, *N Engl J Med* **2005**, *353*, 1685-1693.

[2] a) M. Zambon, J. L. Vincent, *Chest* **2008**, *133*, 1120-1127; b) K. J. Bosma, R. Taneja, J. F. Lewis, *Drugs* **2010**, *70*, 1255-1282; c) A. J. Frank, B. T. Thompson, *Curr Opin Crit Care* **2010**, *16*, 62-68; d) P. A. Efron, A. Martins, D. Minnich, K. Tinsley, R. Ungaro, F. R. Bahjat, R. Hotchkiss, M. Clare-Salzler, L. L. Moldawer, *J Immunol* **2004**, *173*, 3035-3043.

[3] a) M. A. Matthay, R. L. Zemans, *Annu Rev Pathol* **2011**, *6*, 147-163; b) S. Toussaint, H. Gerlach, *N Engl J Med* **2009**, *361*, 2646-2652.

[4] a) T. R. Martin, *J Clin Invest* **2002**, *110*, 1603-1605; b) B. V. Patel, M. R. Wilson, K. P. O'Dea, M. Takata, *J Immunol* **2013**, *190*, 4274-4282; c) R. Bhargava, W. Janssen, C. Altmann, A. Andres-Hernando, K. Okamura, R. W. Vandivier, N. Ahuja, S. Faubel, *PloS one* **2013**, *8*, e61405.

[5] S. Mukhopadhyay, J. R. Hoidal, T. K. Mukherjee, *Respir Res* **2006**, *7*, 125.

[6] a) L. Nespoli, G. Lo Bianco, F. Uggeri, F. Romano, A. Nespoli, D. P. Bernasconi, L. Gianotti, *World J Gastroenterol* **2015**, *21*, 8366-8372; b) B. Rabinow, J. Werling, A. Bendele, J. Gass, R. Bogseth, K. Balla, P. Valaitis, A. Hutchcraft, S. Graham, *Inflammation* **2015**, *38*, 40-60.

[7] B. Kuppast, H. Fahmy, *Eur J Med Chem* **2016**, *113*, 198-213.

[8] A. A. Bekhit, H. T. Fahmy, S. A. Rostom, A. M. Baraka, *Eur J Med Chem* **2003**, *38*, 27-36.

[9] B. Zhou, X. Li, Y. Li, Y. Xu, Z. Zhang, M. Zhou, X. Zhang, Z. Liu, J. Zhou, C. Cao, B. Yu, R. Wang, *ChemMedChem* **2011**, *6*, 904-921.

[10] P. M. Luthra, C. B. Mishra, P. K. Jha, S. K. Barodia, *Bioorg Med Chem Lett* **2010**, *20*, 1214-1218.

[11] M. S. Mohamed, R. Kamel, S. S. Fatahala, *Eur J Med Chem* **2010**, *45*, 2994-3004.

[12] a) Z. Liu, L. Tang, H. Zhu, T. Xu, C. Qiu, S. Zheng, Y. Gu, J. Feng, Y. Zhang, G. Liang, *J Med Chem* **2016**, *59*, 4637-4650; b) G. Chen, Y. Zhang, X. Liu, Q. Fang, Z. Wang, L. Fu, Z. Liu, Y. Wang, Y. Zhao, X. Li, G. Liang, *J Med Chem* **2016**, *59*, 2436-2451; c) Y. Wang, X. Shan, G. Chen, L. Jiang, Z. Wang, Q. Fang, X. Liu, J. Wang, Y. Zhang, W. Wu, G. Liang, *Br J Pharmacol* **2015**, *172*, 4391-4405; d) P. Yu, L. Dong, Y. Zhang, W. Chen, S. Xu, Z. Wang, X. Shan, J. Zhou, Z. Liu, G. Liang, *Eur J Med Chem* **2015**, *94*, 436-446.

[13] J. Hu, Y. Wang, X. Wei, X. Wu, G. Chen, G. Cao, X. Shen, X. Zhang, Q. Tang, G. Liang, X. Li, *Eur J Med Chem* **2013**, *64*, 292-301.

[14] a) Y. Shi, J. Zhang, N. Grazier, P. D. Stein, K. S. Atwal, S. C. Traeger, S. P. Callahan, M. F. Malley, M. A. Galella, J. Z. Gougoutas, *J Org Chem* **2004**, *69*, 188-191; b) S. Kolb, O. Mondesert, M. L. Goddard, D. Jullien, B. O. Villoutreix, B. Ducommun, C. Garbay, E. Braud, *ChemMedChem* **2009**, *4*, 633-648.

[15] M. M. Abdel-Atty, N. A. Farag, S. E. Kassab, R. A. Serya, K. A. Abouzid,

Bioorg Chem **2014**, *57*, 65-82.

[16] a) M. Rossol, H. Heine, U. Meusch, D. Quandt, C. Klein, M. J. Sweet, S. Hauschildt, *Crit Rev Immunol* **2011**, *31*, 379-446; b) C. Alexander, E. T. Rietschel, *J Endotoxin Res* **2001**, *7*, 167-202.

[17] a) K. N. Iskander, M. F. Osuchowski, D. J. Stearns-Kurosawa, S. Kurosawa, D. Stepien, C. Valentine, D. G. Remick, *Physiol Rev* **2013**, *93*, 1247-1288; b) P. Shukla, G. M. Rao, G. Pandey, S. Sharma, N. Mittapelly, R. Shegokar, P. R. Mishra, *Br J Pharmacol* **2014**, *171*, 5011-5031.

[18] R. R. Bell, V. K. Nonavinakere, M. R. Soliman, *Toxicol Lett* **2000**, *114*, 101-109.

[19] J. Grommes, O. Soehnlein, *Mol Med* **2011**, *17*, 293-307.

[20] N. Bagul, S. Roy, A. Ganjre, R. Kathariya, A. Meher, P. Singh, *J Clin Diagn Res* **2016**, *10*, ZC81-84.

[21] a) W. J. Zhang, B. Frei, *Mediators Inflamm* **2015**, *2015*, 274314; b) C. A. Martin, M. E. Dorf, *Cell Immunol* **1991**, *135*, 245-258.

[22] S. G. Royce, Y. Moodley, C. S. Samuel, *Pharmacol Ther* **2014**, *141*, 250-260.

Abbreviations

LPS, Lipopolysaccharides; ALI, Acute lung injury; ELISA, Enzyme linked immunosorbent assay; MPMs, Mouse primary peritoneal macrophages; BALF, Bronchoalveolar lavage fluid; CD68, Cluster of Differentiation 68; VCAM-1, Vascular cell adhesion molecule 1; ICAM-1, Intercellular Adhesion Molecule 1.

Figure Legends

Table 1. Anti-inflammatory screening of compounds 11a-o.

Table 2. Anti-inflammatory screening of compounds 12a-i.

Figure 1. Structures of 1−6 with thiazolo and pyrimidine fused heterocyclic ring-systems.

Figure 2. Plots of predicted activity against the corresponding experimental activity on IL-6 inhibition. N, the number of compounds taken into account in the regression; R^2, the multiple correlation coefficient; R_{adj}^2, adjusted multiple correlation coefficient; s, residual standard error; and the F value is related to the F-statistic analysis (Fischer test). The numbers in parentheses mean the standard deviation of the coefficients. (A) IR_{IL-6}= 103.0571 (±24.4099) + 21.9904 (±5.7686) MoRSEE10 + 5.9199 (±0.9759) RDFM12 - 6.7264 (±1.4819) RDFM8, N=24, R^2=0.7643, R_{adj}^2=0.7289, s=14.96, $F_{3, 20}$=21.62, p=1.737^{-6}; (B) $IR_{TNF-\alpha}$= -144.107 (±30.726)-115.138 (±19.247) MoRSEC1+40.129 (±7.044) MoRSEE10 + 31.139 (±6.869) MoRSEE7, N=24, R^2=0.7634, R_{adj}^2=0.7279, s=11.45, $F_{3, 20}$=21.51, p=1.804^{-6}.

Figure 3. Active compounds inhibited LPS-induced inflammatory cytokines in a dose-dependent manner. Mouse primary peritoneal macrophages (MPMs) were pretreated with vehicle or compounds at indicated concentrations (1, 2.5, 5 and 10 μM) for 30 min. Then, cells were incubated with LPS (0.5 μg/mL) for 24 h. IL-6 and TNF-α levels in the culture medium were measured by ELISA and were normalized to the total protein amount. (A) IL-6 levels measured by ELISA. (B) TNF-α levels measured by ELISA. Each bar represents mean ± SEM of 3 independent. Statistical significance relative to the LPS group was indicated, *p < 0.05, **p < 0.01, ***p < 0.001 vs LPS vehicle.

Figure 4. Effect of 11e and 11l pretreatment on survival rate in mice after LPS administration. Compounds were dissolved with 0.1% sodium carboxyl methyl cellulose (CMC-Na). Male ICR mice were pretreated with 11e, 11l or vehicle for seven days by intragastric administration (20 mg/kg/day), followed by the injection of LPS (i.v., 20 mg/kg). The survival rate was recorded for 7 days at an interval of 12 h after the LPS injection; n = 10 animals in each group, *p < 0.05, **p < 0.01vs LPS

vehicle.

Figure 5. 11e and 11l ameliorated histopathological changes of lung in LPS stimulated ALI mice. Male B6 mices were given an intragastric administration of compounds (10 or 20 mg/kg/day) or 1% CMC-Na 7 days prior to an intratracheal administration of LPS (5 mg/kg), then mice were anaesthetized and killed at 6 h after LPS challenged. Bronchoalveolar lavage fluid and lung tissues were collected for further tests. (A) The lung W/D ratio. (B) The total number of cells in BALF. (C) Quantification of CD68 staining. (D) CD68-immunostained macrophage in the lung sections (red, ×400). (E) H&E staining (×400). *p < 0.05, **p < 0.01 , ***p < 0.001 vs LPS vehicle.

Figure 6. Attenuation of acute LPS-induced pulmonary inflammation by 11e and 11l. (A) The relative amount of IL-6 in BALF. (B) The relative amount of TNF-α in BALF. (C) The relative amount of IL-6 in serum. (D) The relative amount of TNF-α in serum. Statistical significance relative to the LPS group was indicated, ns: no significance, *p < 0.05, **p < 0.01, ***p < 0.001 vs LPS vehicle.

Figure 7. 11e and 11l inhibited the inflammatory genes expression induced by LPS in mouse lung tissue. (A)) IL-1β, (B) IL-6, (C) TNF-α, (D) VCAM-1, (E) ICAM-1. ns: no significance, *p < 0.05, **p < 0.01, ***p < 0.001 vs LPS vehicle.

Scheme 1. General synthetic route of thiazolo [3, 2-a] pyrimidine derivatives 11a-o.
[a]Reagents and conditions: (a) sulfamic acid, EtOH, 78 ºC, 4 h, 90−95%; (b) ethyl 2-chloroacetate, pyridine, EtOH, 78 ºC, 3 h; (c) 4-morpholinobenzaldehyde, morpholine, EtOH, 78 ºC, 6 h, 35−60%.
Scheme 2. General synthetic route of thiazolo [3, 2-a] pyrimidine derivatives 12a-i.
[b]Reagents and conditions: (a) sulfamic acid, EtOH, 78 ºC, 4 h, 90−95%; (b) ethyl 2-chloroacetate, pyridine, EtOH, 78 ºC, 3 h; (c) aldehydes 10a-10i, morpholine, EtOH, 78 ºC, 6 h, 35−60%.

10.1002/cmdc.201700175

Table 1.

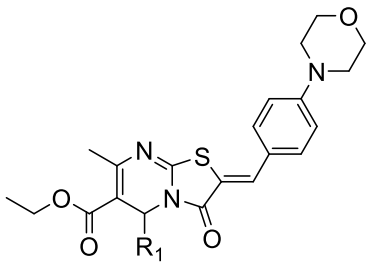

11a-o

Compd	R^1	(%) inhibition (10 μM)[a] IL-6	TNF-α
6	phenyl	81.78 ± 4.33***	59.76 ± 7.06***
11a	(4-Br)phenyl	75.68 ± 7.34***	56.71 ± 8.79***
11b	(4-F)phenyl	80.25 ± 6.03***	54.30 ± 7.95***
11c	(3,4-diOCH_3)phenyl	70.62 ± 6.61***	61.80 ± 19.11**
11d	(4-OCH_2CH_3)phenyl	66.26 ± 16.92***	57.97 ± 8.35***
11e	4-(allyloxy)phenyl	92.82 ± 1.13***	65.96 ± 6.28***
11f	(4-OH)phenyl	67.92 ± 7.86***	68.57 ± 3.77***
11g	(3-OH)phenyl	45.97 ± 2.78***	52.60 ± 7.58***
11h	(4-OH-3-OCH_3)phenyl	19.88 ± 4.76 ns	48.02 ± 6.21***
11i	(3,4-diOH)phenyl	79.30 ± 1.16***	71.45 ± 6.21***
11j	(4-CH_3)thiazol-5-yl	37.29 ± 2.16***	44.31 ± 8.18***
11k	(5-CH_3)furan-2-yl	36.83 ± 1.61***	40.19 ± 5.88**
11l	thiophen-2-yl	94.75 ± 0.24***	65.67 ± 5.59***
11m	cyclopropyl	63.07 ± 5.42***	53.16 ± 8.25***
11n	propyl	54.82 ± 0.85***	62.04 ± 6.11***
11o	cyclohexyl	34.69 ± 2.46**	49.42 ± 2.10***

[a]Values are mean of at least n = 3 independent experiments ± SEM

10.1002/cmdc.201700175

Table 2.

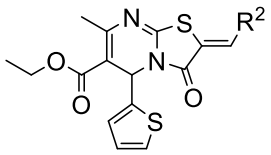

12a-i

Compd	R^2	(%) inhibition (10 μM)[c]	
		IL-6	TNF-α
11l	4-morpholin-phenyl	85.50 ± 2.50***	58.67 ± 3.18***
12a	4-(4-CH_3-piperazine)-phenyl	5.50 ± 0.50 ns	7.66 ± 0.88 ns
12b	4-$N(CH_3)_2$-phenyl	9.33 ± 3.84 ns	23.67 ± 8.95*
12c	4-(pyrrolidin)-phenyl	12.00 ± 1.15 ns	17.67 ± 2.18*
12d	4-$N(CH_2CH_3)_2$-phenyl	20.67 ± 8.68 ns	76.33 ± 2.84**
12e	4-(NCH_3-$(CH_2)_2$-$N(CH_3)_2$)-phenyl	31.67 ± 12.77 **	59.50 ± 5.50***
12f	5-CH_3-furan-2-yl	39.33 ± 19.19**	7.33 ± 1.33 ns
12g	pyrrol-2-yl	61.67 ± 1.45***	23.67 ± 2.96**
12h	4-($O(CH_2)_3$-$N(CH_3)_2$)-phenyl	ND[a]	ND
12i	phenyl	NA[b]	NA

[a]ND means not detected

[b]NA means no activity

[c]Values are mean of at least n = 3 independent experiments ± SEM

10.1002/cmdc.201700175

Figure 1.

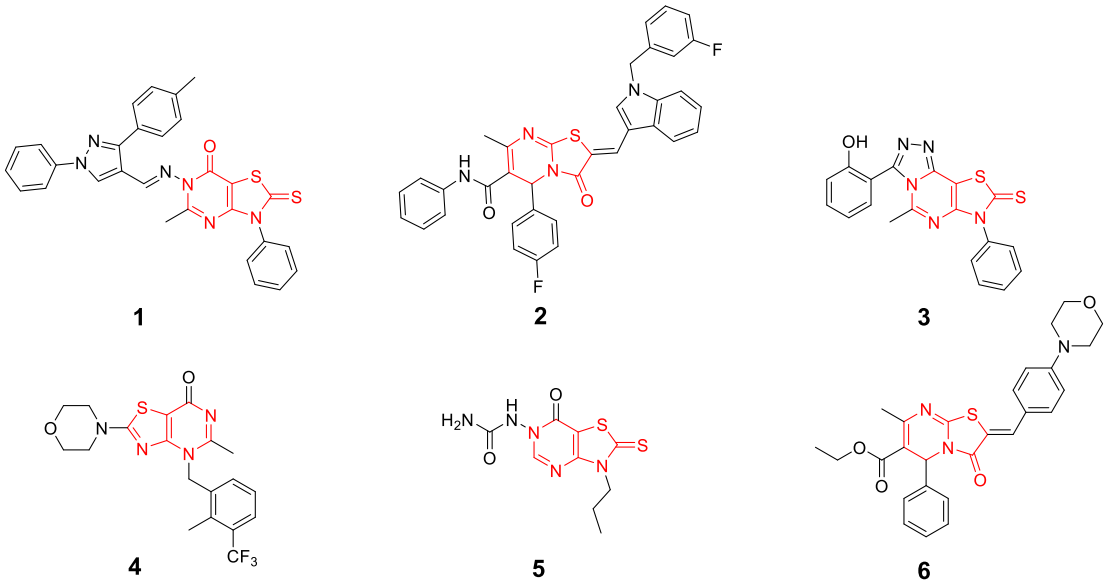

Figure 2.

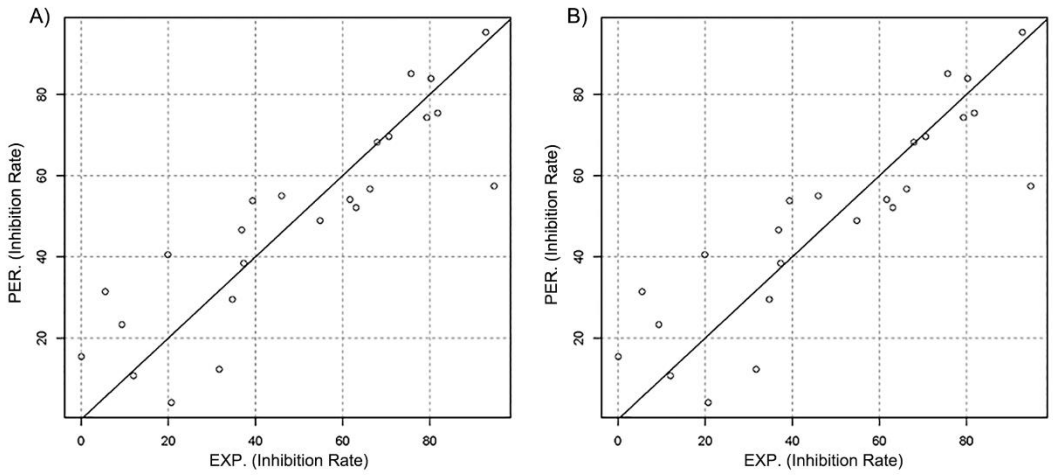

10.1002/cmdc.201700175

Figure 3.

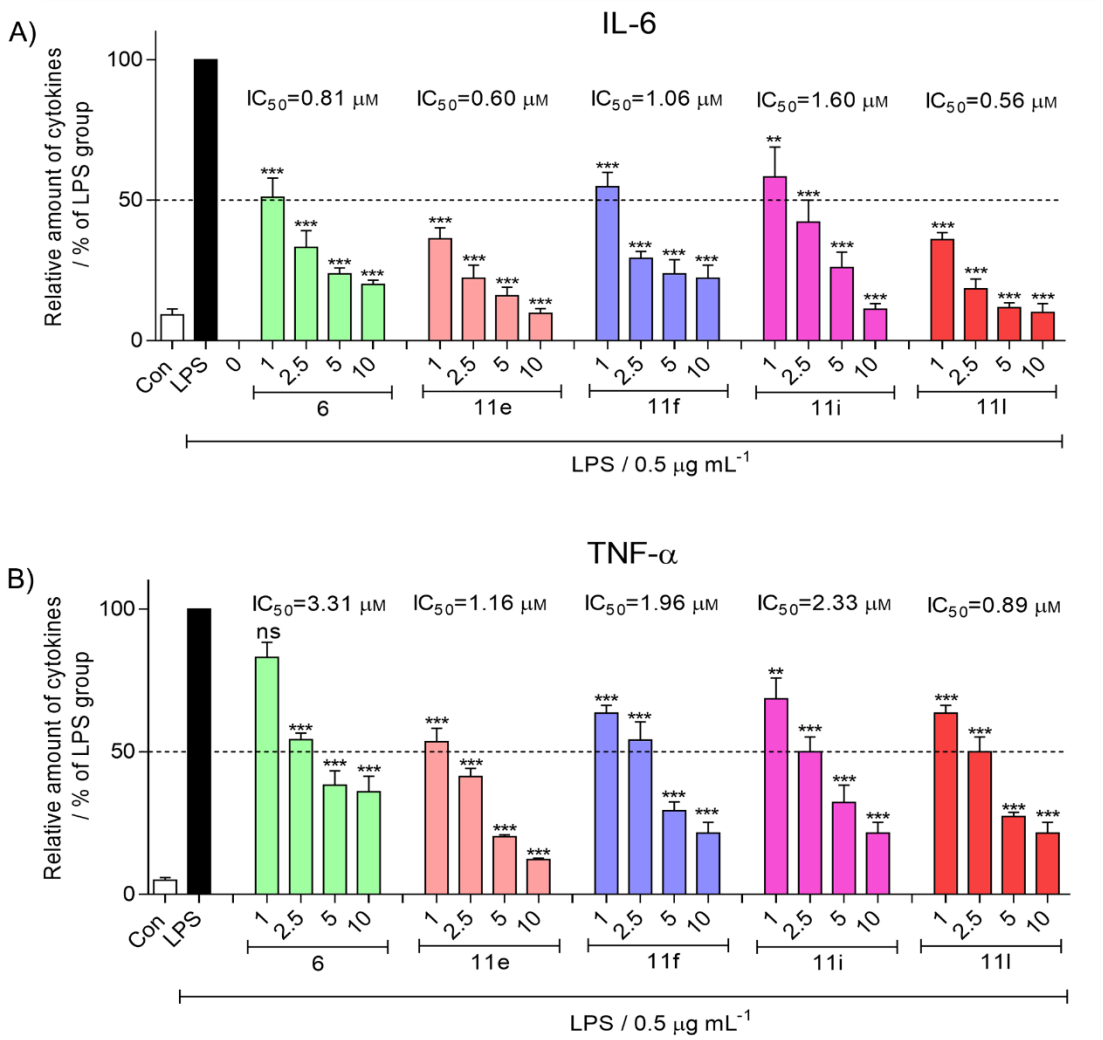

Figure 4.

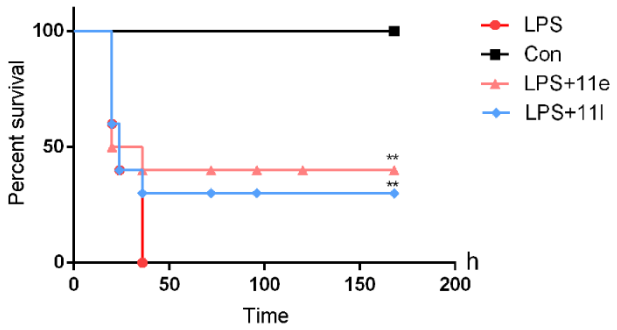

10.1002/cmdc.201700175

Figure 5.

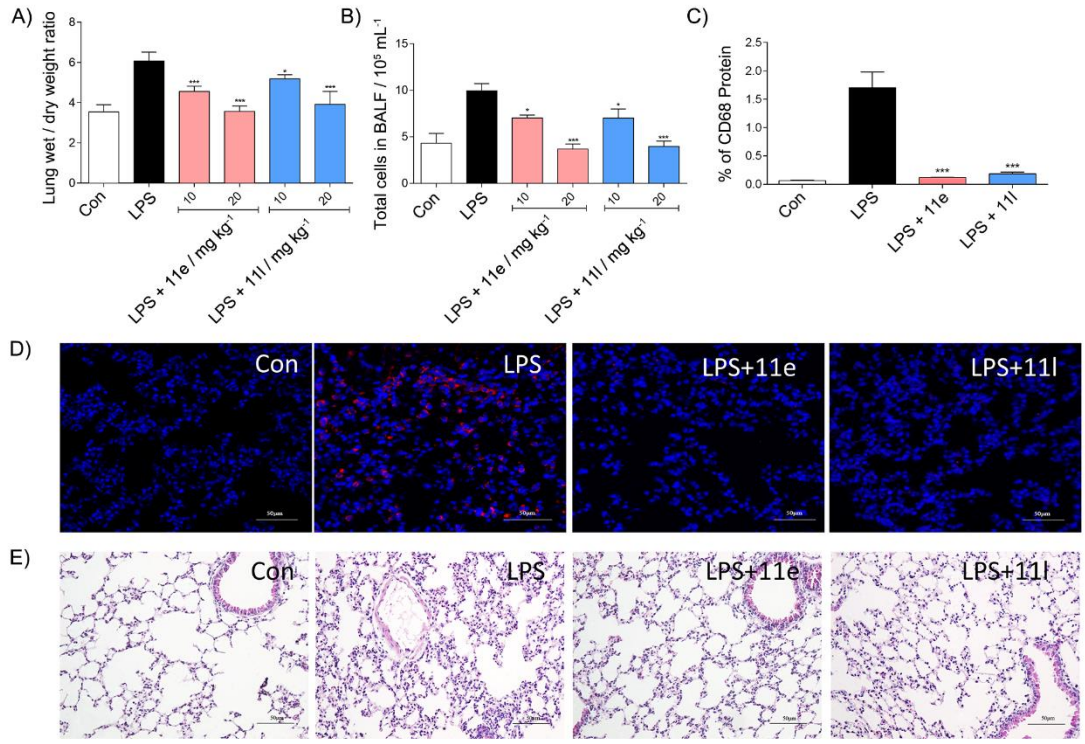

Figure 6.

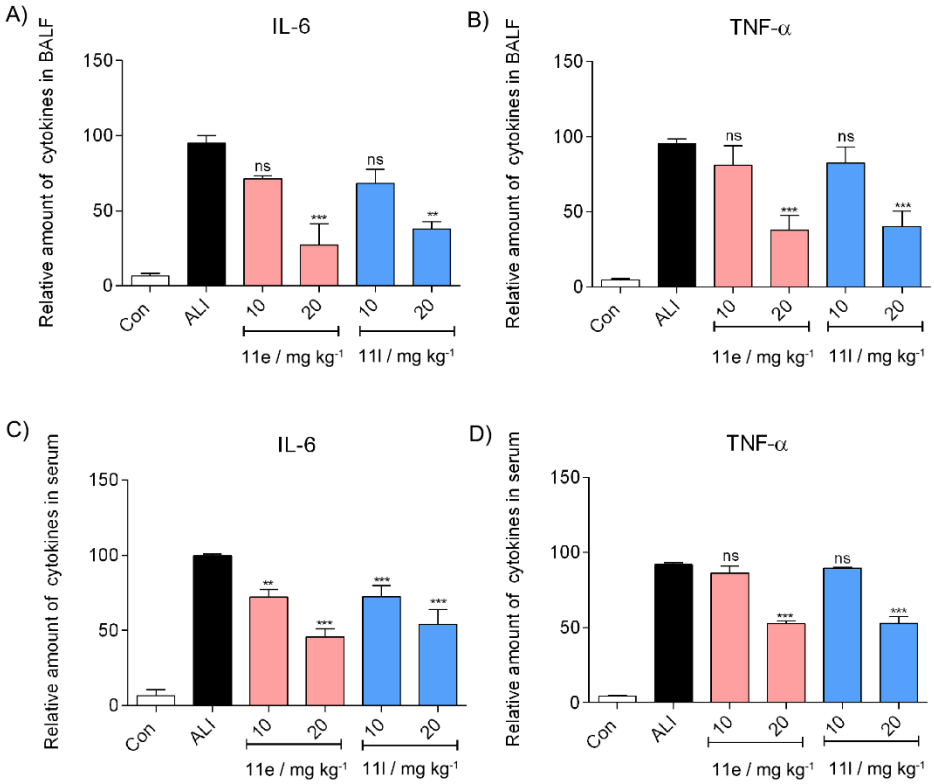

10.1002/cmdc.201700175

Figure 7.

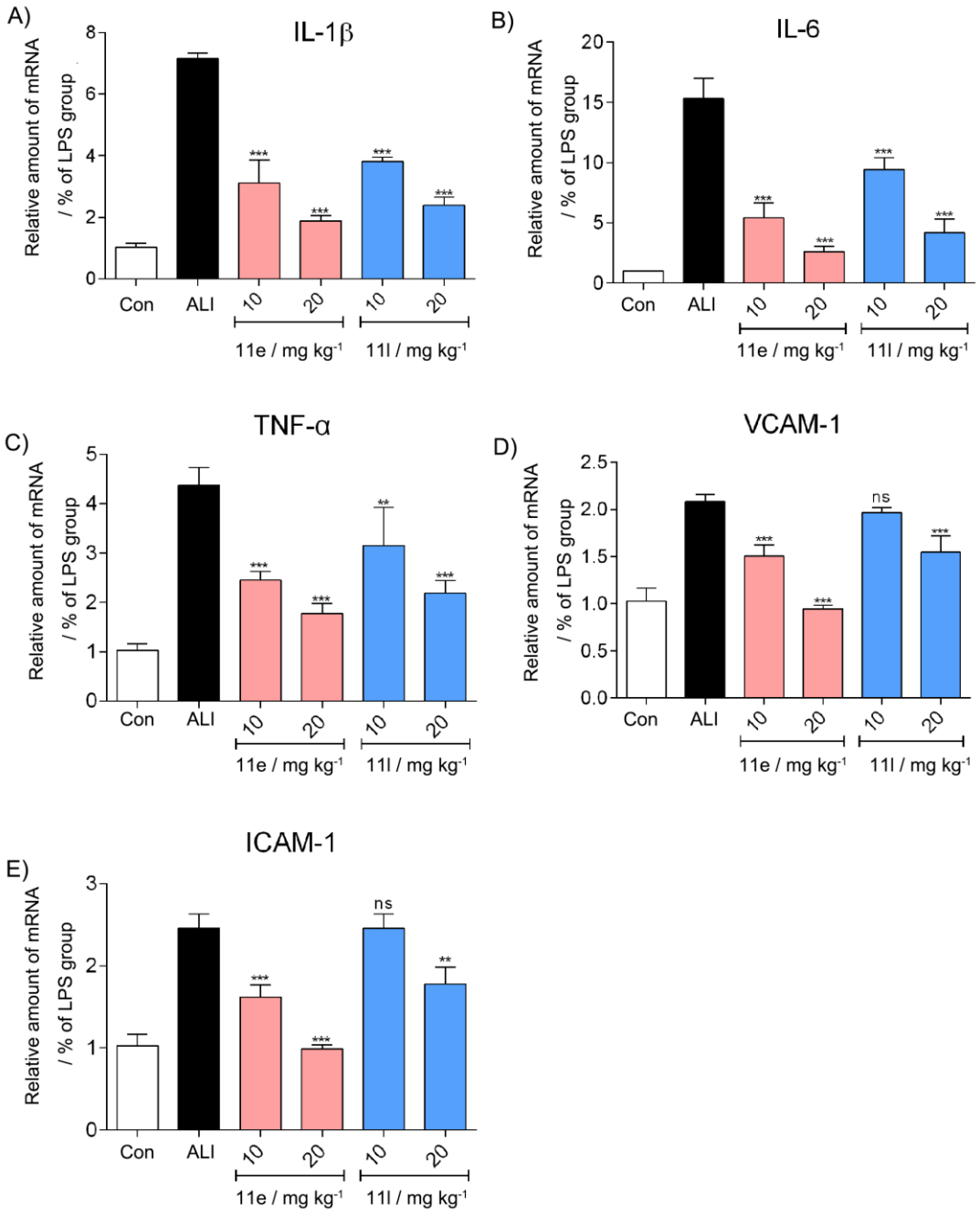

10.1002/cmdc.201700175

Scheme 1.

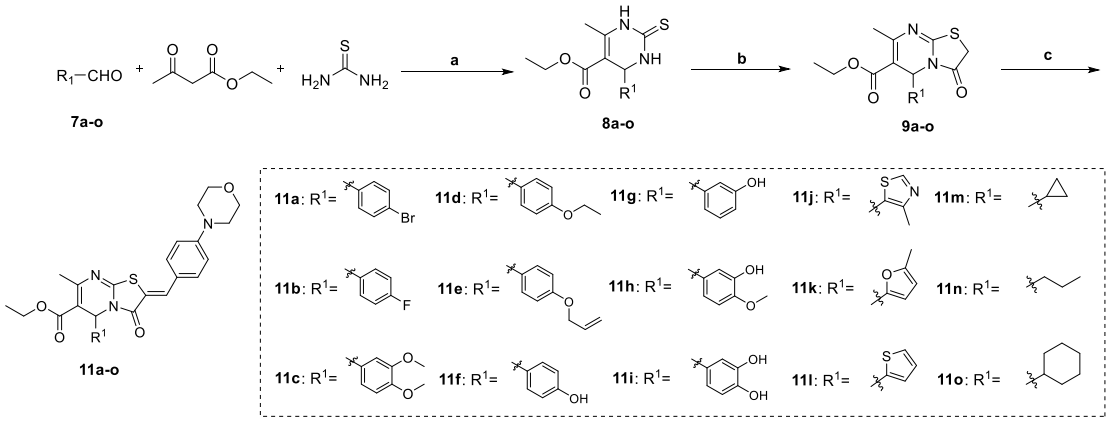

Scheme 2.

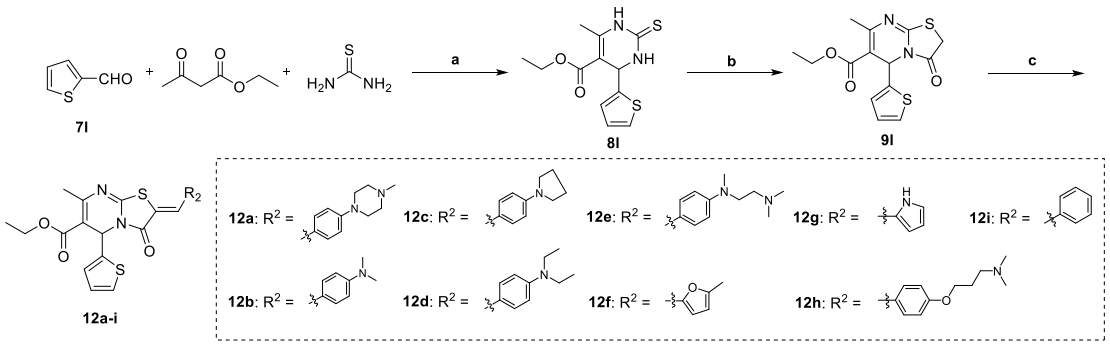

10.1002/cmdc.201700175

Graphical Abstract

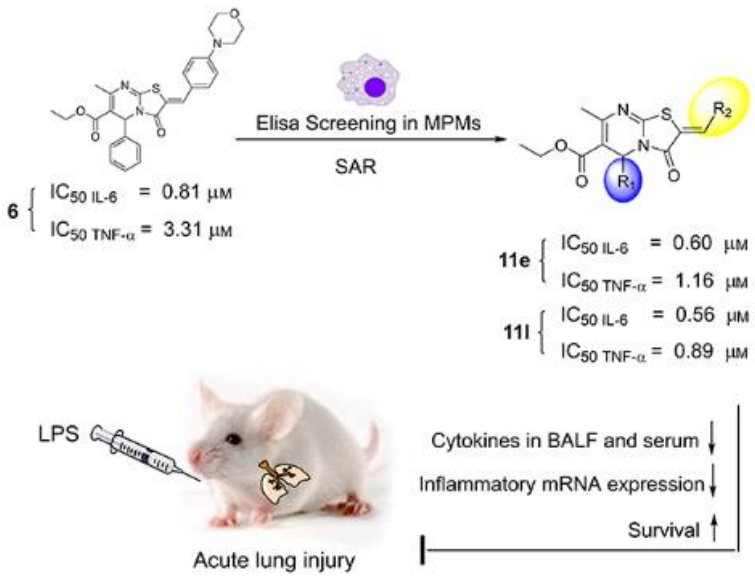

Text for Table of Contents: Based on lead compound **6**, we designed and synthesized a series of thiazolo[3,2-a]pyrimidine derivatives. The most promising compounds **11e** and **11l** inhibited LPS-induced cytokines with low IC_{50}. Further administration of them attenuated LPS-caused acute lung injury *in vivo*.